

Mn DOPED SnO₂ PREPARED BY A SOL-GEL METHOD

Ana-Maria UNGUREANU¹, Ioana JITARU², Florinela GOSNEA³

Mn doped tin dioxide nanoparticles (with 2, 4, 6% at. Mn) for possible diluted magnetic semiconductors (DMS) applications were successfully obtained through a facile ethylene glycol assisted sol-gel process. All samples were characterized through XRD and TG/DSC analysis, UV-VIS and FTIR spectroscopy. TG/DSC analysis results suggest an optimal thermal treatment temperature of 500°C. XRD results confirm the formation of Mn doped tin dioxide nanocrystallites in accordance with thermogravimetric results. For all the samples no secondary phases were observed, indicating a good Mn integration in the tin dioxide lattice. Crystallite sizes were calculated with Scherrer's equation; values of 6 nm were obtained. Band gap energies were estimated with Tauc method and compared with the value of an undoped sample, showing a decrease in the Eg value that emphasizes the increase in dopant concentration.

Keywords: tin dioxide; DMS; sol-gel; ethylene glycol

1. Introduction

Diluted magnetic semiconductors (DMS) are materials that possess the characteristics of semiconductors, as well as magnetic properties. The studies regarding oxide based DMSs have escalated since the prediction of room temperature ferromagnetism in 5% Mn doped ZnO by Dietl et al. [1]. Given this point, simple oxides like SnO₂ [2-17], ZnO [20-27], TiO₂ [28, 29] or mixed oxides [30-34] captured scientists' attention.

Tin dioxide is a wide band gap semiconductor, with many potential applications: photocatalyst, sensor, electronic material. It is also a good DMS candidate due to its doping potential with several transition metals (Fe, Co, Ni, Mn) [2-16] or rare earths metals (Dy, Eu, Er) [17]. Depending on the desired properties, a vast number of synthesis routes are available in literature: spray pyrolysis [3], pulsed laser deposition [5, 16], polymeric precursor method [9], co-precipitation [10, 11], solid-state synthesis [12, 15], various sol-gel approaches [2, 7, 8, 13, 18]. The sol-gel process seems to be far more investigated than other

¹ PhD stud., Dept. of Inorganic Chemistry, Physical Chemistry and Electrochemistry, University POLITEHNICA of Bucharest, Romania, e-mail: annaungureanu@yahoo.com

² Prof., Dept. of Inorganic Chemistry, Physical Chemistry and Electrochemistry, University POLITEHNICA of Bucharest, Romania

³ Student, Faculty of Applied Chemistry and Materials Science, University POLITEHNICA of Bucharest, Romania

routes due to its numerous advantages: low cost, non-toxic precursors, good control over experimental parameters, good homogeneity and good size control.

Given the large number of recent publications on doped tin dioxide, we notice that there are still many discrepancies regarding the results on Mn doped SnO_2 . The reported crystallite sizes vary from 7 to 70 nm, depending on the synthesis method. Also, there are inconsistencies regarding the solubility limit of Mn ions in the SnO_2 lattice: Fitzgerald et al [6] report a solubility limit of 5%, Azam et al [18] states that at 15% no secondary phases are formed, and Kimura et al [5] reports a solubility limit as high as 34%, although they mention the fact that the solubility limit may be pushed upwards through PLD method. Xiao et al report room temperature ferromagnetism for Mn doped SnO_2 thin films, while Gao et al [19] found no RTFM in their studies.

In this study, we investigate the structural characteristics of Mn doped SnO_2 (0.02, 0.04, 0.06) synthetized through a simple ethylene glycol assisted sol-gel method.

We aim to determine an optimal heat treatment and the solubility limit of Mn ions into the host tin dioxide lattice. Optical properties of doped samples are discussed.

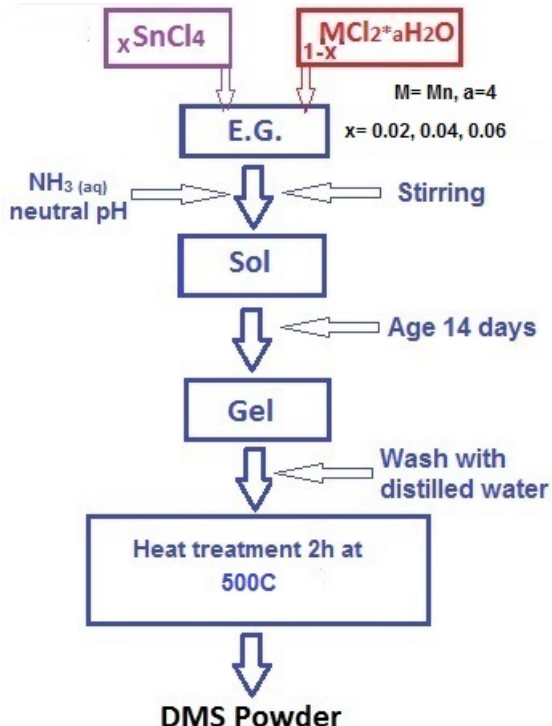
2. Experimental procedure

Manganese doped tin dioxide nanoparticles were obtained by a simple ethylene glycol assisted sol-gel method, presented in Fig. 1. The 2%, 4% and 6% at. Mn doped samples were obtained using SnCl_4 (99.99%) and $\text{MnCl}_2 \cdot 4\text{H}_2\text{O}$ salts. The salts were mixed in ethylene glycol under magnetic stirring. Concentrated ammonia (25% wt.) was added under stirring drop wise until a neutral pH was reached. The samples were kept under stirring for another 30 minutes, to make sure that the sol is properly formed. All three samples were left to age in laboratory conditions for 14 days. The creamy coloured gels were washed with distilled water in order to remove residual ions like Cl^- . The gels were subjected to a thermal treatment carried out at 500°C for 2 hours.

TG/DSC thermograms (20°C-900°C) of the Mn doped samples were recorded on a Netzsch STA Jupiter 449 apparatus, using an open alumina crucible, in a dynamic air atmosphere, 20 mL/minute, with a heating rate of 10K/minute.

X-ray powder diffraction patterns were obtained with a Shimadzu XRD6000 diffractometer, using $\text{Cu K}\alpha$ (1.5406 Å) radiation operating with 30 mA and 40 kV in the 2 θ range 10–70°. A scan rate of 1° min^{-1} was employed.

UV-Vis diffuse reflection spectra were recorded between 200-900 nm, on Able Jasco V560 spectrometer, with a scanning rate of 200 nm/minute.

Fig. 1 - Synthesis scheme of Mn doped SnO₂

FTIR absorption spectra were recorded using a Bruker Tensor 27 device, within 4000-400 cm⁻¹ range.

3. Results and Discussion

3.1. Thermogravimetric analysis

The thermograms of the 2% and 6% at. Mn doped gels were obtained in order to determine an optimal heat treatment (figure 2). As expected, both samples exhibit similar thermal patterns, in accordance with the chosen synthesis route.

The weight loss around 100°C, accompanied by an endothermic effect on the DSC curve is attributed to the elimination of physically bond water. Both samples exhibit important weight losses between 110°C-500°C, along with exothermic effects on the DSC curve. These losses are explained by the elimination of NH₄⁺ ions, and the decomposition of the organic remains. The difference in the magnitude of DSC effects can be attributed to the Mn influence on the thermal decomposition. At temperatures higher than 500°C, both samples are thermally stable in the studied temperature range. Based on the information

gathered through TG/DSC analysis, the gels were thermally treated at 500°C for 2 hours with a heating rate of 10°C/minute.

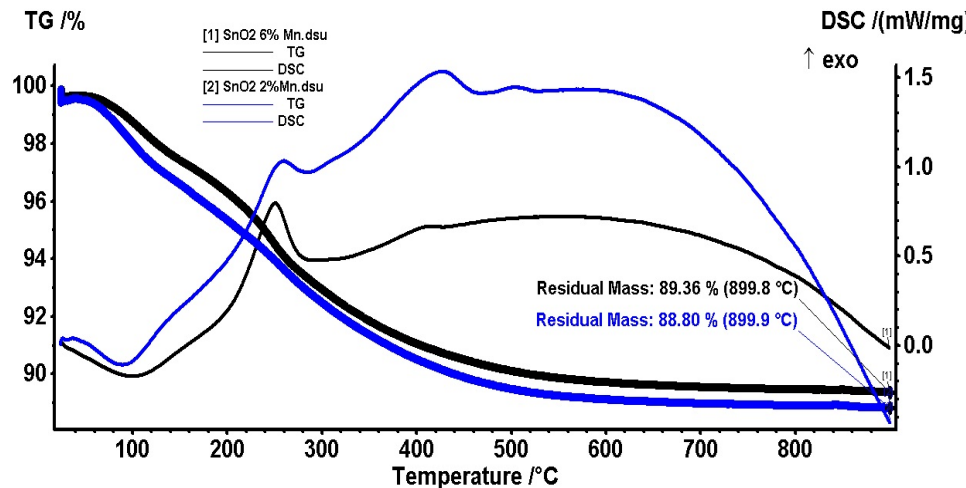


Fig. 2 - Thermograms of 2% (coloured line) and 6% (black line) Mn doped SnO₂ gels

3.2. X Ray Diffraction

The XRD patterns recorded for the three doped tin dioxide samples are presented in Fig. 3, in comparison with an undoped SnO₂ sample. All diffractograms are characteristic to rutile type SnO₂ in accordance with ASTM 41-1445, and with our reference SnO₂ sample, obtained through the same synthesis route.

For all three Mn concentrations, all peaks are clearly indexed to tetragonal SnO₂. No secondary phases are observed, indicating a good Mn integration in the tin dioxide lattice. This suggests that through the ethylene-glycol assisted sol-gel synthesis the solubility limit of manganese ions into the tin dioxide lattice exceeds 6% at. in agreement with literature [9,15]. A slight displacement in 2 theta values is observed for all samples, suggesting that the dopant was successfully integrated in the host lattice.

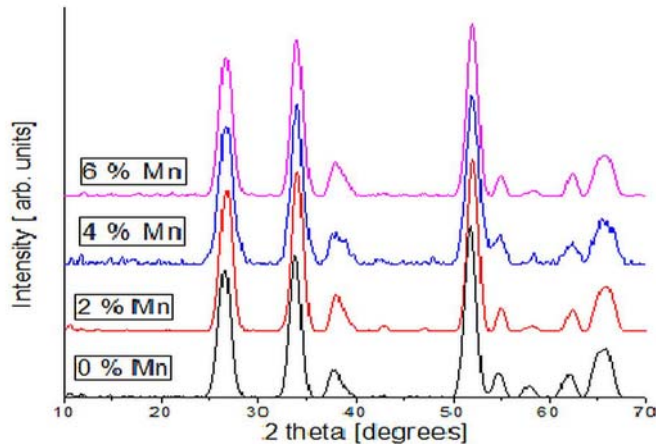


Fig. 3 - Mn doped tin dioxide XRD patterns in comparison with undoped sample

Table I contains the structural and dimensional characteristics of all Mn doped samples, in comparison with an undoped tin dioxide nanopowder. The crystallite size was calculated using Scherrer's equation. The difference between the crystallite size of the undoped sample and the crystallite size of the doped samples is less than 0.5nm. No size variations are observed with dopant concentration as all samples were calculated to have a size of 6 nm.

Table I
Crystallite size and cell parameters calculated for Mn doped tin dioxide in comparison with undoped tin dioxide

Mn concentration [%]	Crystallite size [nm]	Cell Parameters [Å]	
		a	c
0	5.6	4.73	3.19
2	6	4.70	3.17
4	6	4.70	3.17
6	6	4.70	3.17

Cell parameters of all doped samples have lower values than the undoped sample. All doped samples were calculated to have similar lattice parameters values. The minor differences that are observed may be associated with the distortions that occur during the incorporation of smaller manganese ions into the tin dioxide lattice.

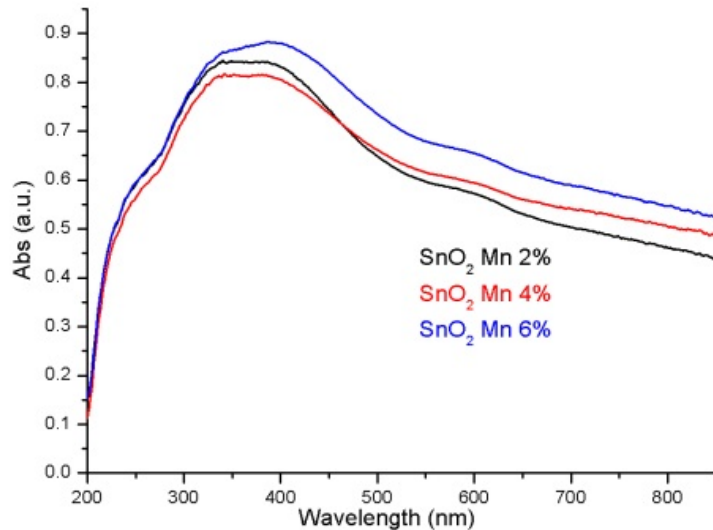
3.3. UV-VIS spectroscopy

UV-VIS spectra for all three doped samples are presented in Fig. 4. It can be clearly observed that all three samples have the typical spectrum of SnO_2 , with a large absorption band around 380 nm and a shoulder at 250nm. The broad shoulder from 600nm can be attributed to the manganese ions.

Table II

Band gap energies calculated with Tauc method

Mn concentration [%]	Eg [eV]
0	3.03
2	2.48
4	2.38
6	2.33

Fig. 4 - UV-VIS spectra obtained for 2%, 4% and 6% at. Mn doped SnO_2 nanoparticles

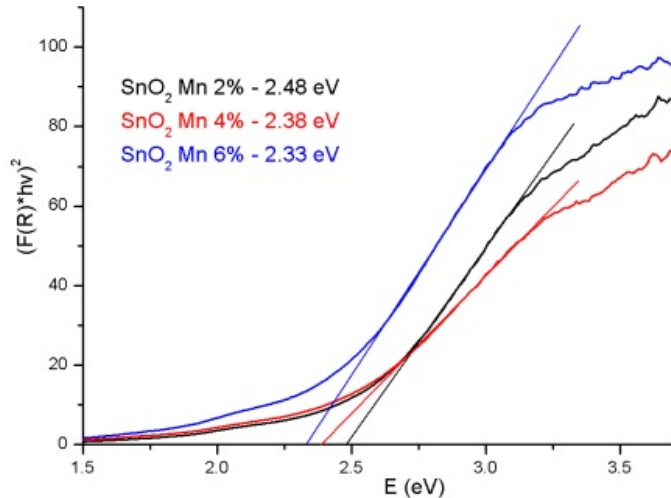


Fig. 5 - Tauc plot of $(F(R)*h\nu)^2$ vs photon energy

Band gap energies were calculated through Tauc's method (Fig. 5) and were compared with the band gap value for undoped tin dioxide, calculated through the same method (table II) [35]. While comparing the E_g values of undoped and doped samples, a significant decrease is observed. This decrease is more obvious with the increase of Mn concentration. We assign this behaviour to the occurrence of additional electronic levels inside the band gap, as a consequence of Mn incorporation in the SnO₂ lattice.

3.4. FT-IR Spectroscopy

To obtain more details regarding the structure of Mn doped SnO₂, FT-IR analysis was performed on all doped samples, their spectra being shown in figure 6. The peak at 1627 cm^{-1} corresponds to water molecules adsorbed from the environment. It can be clearly seen that all samples showed similar spectra, with typical rutile type SnO₂ peak 615 cm^{-1} . This band is assigned to fundamental Sn-O vibration, with Sn-O-Sn in antisymmetric stretching mode [36- 38]. The inset shows that the main peak exhibits one left shoulder at 680 cm^{-1} , whose signal belongs to O-Sn-O vibration [39, 40], and two right shoulders, at 508 cm^{-1} and 470 cm^{-1} that are also characteristic to Sn-O vibration [41]. No Mn-O characteristic peaks were observed because the Mn-O vibration is masked by the stronger Sn-O vibration, as both bonds vibrate in the same wavenumbers interval [42-44].

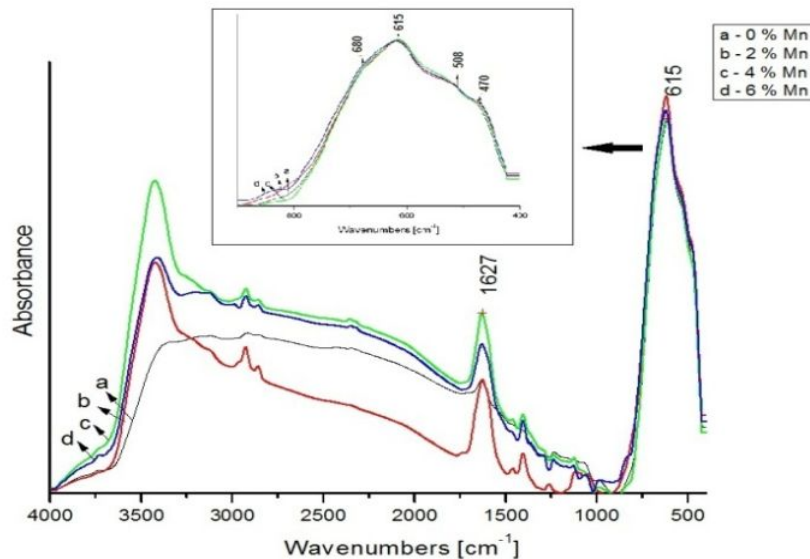


Fig. 6 - FTIR spectra for 2%, 4% and 6% at. Mn doped SnO_2 , in comparison with a previously obtained undoped SnO_2 sample

4. Conclusions

Tin dioxide powders containing nanocrystallites doped with 2, 4, and 6% at. Mn were obtained through an ethylene glycol assisted sol-gel method. The thermal treatment conducted on all samples was performed in accordance with TG/DSC results, which suggest that a good calcination may be carried at 500°C . XRD confirms the formation of nanostructured SnO_2 , with a rutile type structure, with small crystallite size, of 6 nm. Tin dioxide easily incorporates Mn ions up to 6% concentration, when no secondary phases are observed, suggesting that at this concentration, the Mn solubility into the host lattice is not reached. UV-VIS spectra obtained for all three samples are characteristic to tin dioxide. Mn presence in the tin dioxide lattice does not significantly influence the shape of UV-VIS spectra. The calculated band gap energies decrease with the increase of dopant concentration, as a result of the occurrence of additional energetic levels in the forbidden band.

Acknowledgements

The work has been funded by the Sectoral Operational Programme Human Resources Development 2007-2013 of the Romanian Ministry of Labour, Family and Social Protection through the Financial Agreement POSDRU/107/1.5/S/76903.

R E F E R E N C E S

- [1] *T. Dietl, H. Ohno, F. Matsukura, J. Cibert, D. Ferrand*, Science 287, 1019 (2000)
- [2] *K. Gopinadhan, Subhash C. Kashyap, Dinesh K. Pandya, and Sujeet Chaudharya*, Journal of Applied Physics 102, 113513, 2007
- [3] *K. Vadivel, V. Arivazhagan, S. Rajesh*, Research Volume 2, Issue 4, April-2011 ISSN 2229-5518
- [4] *R. Brahma, M. G. Krishna and A. K. Bhatnagar*, Bull. Mater. Sci., 29(3), 2006, 317–322.
- [5] *H. Kimura, T. Fukumura, M. Kawasaki, K. Inaba, T. Hasegawa et al*, Appl. Phys. Lett. 80, 94 (2002);
- [6] *C. B. Fitzgerald, M. Venkatesan, A. P. Douvalis, S. Huber, and J. M. D. Coey*, Journal of Applied Physics 95(11), 2004
- [7] *S. Gnanam, V. Rajendran*, J Sol-Gel Sci Technol (2010) 53:555–559
- [8] *L. Jiang, G. Sun, Zhenhua Zhou, Shiguo Sun et al*, J. Phys. Chem. B 2005, 109, 8774-8778
- [9] *R. Parra, L.A. Ramajo, M.S. Góes, J.A. Varela, M.S. Castro*, Materials Research Bulletin 43 (2008) 3202–3211
- [10] *H. Bastami, E. Taheri-Nassaj*, Journal of Alloys and Compounds 495 (2010) 121–125
- [11] *Z.M. Tian, S.L. Yuan, J.H. He, P. Li*, Journal of Alloys and Compounds 466 (2008) 26–30
- [12] *Sunita Mohanty, S. Ravi*, Solid State Communications 150 (2010) 1570–1574
- [13] *Y. Xiao, Shihui Ge, Li Xi, Yalu Zuo et al*, Applied Surface Science 254(22), 2008, 7459–7463
- [14] *L. B. Duan, G. H. Rao, J. Yu, Y. C. Wang, G. Y. Liu, and J. K. Liang*, J. Appl. Phys. **101**, 063917 (2007);
- [15] *K.H. Gao, Z.Q. Li, X.J. Liu, W. Song, H. Liu, E.Y. Jiang*, Solid State Communications 138 (2006) 175–178
- [16] *Yanxue Chen and Jun Jiao*, International Journal of Modern Physics B Vol. 23, Nos. 6 & 7 (2009) 1904–1909
- [17] *K. Mohan Kant, K. Sethupathi and M. S. Ramachandra Rao*, International Symposium of Research Students on Materials Science and Engineering December 20-22, 2004, Chennai, India
- [18] *A. Azam, Arham S. Ahmed, M. Chaman, and A. H. Naqvi*, J. Appl. Phys. 108, 094329 (2010);
- [19] *K.H. Gao, Z.Q. Li, X.J. Liu, W. Song, H. Liu, E.Y. Jiang*, Solid State Communications 138 (2006) 175–178
- [20] *Santi Maensiri, Jakkapon Sreesongmuang, Chunpen Thomas, Jutharatana Klinkaewnarong*, Journal of Magnetism and Magnetic Materials 301 (2006) 422–432
- [21] *Shengqiang Zhou, K. Potzger, Qingyu Xu, G. Talut, M. Lorenz et al*, Vacuum 83 (2009) S13–S19
- [22] *Y. Kalyana Lakshmia, K. Srinivas, B. Sreedharb et al*, Materials Chemistry and Physics 113 (2009) 749–755
- [23] *Yingjing Jiang, Wei Wang, Chengbin Jing, Chunyue Cao, Junhao Chu*, Materials Science and Engineering B xxx (2011) xxx–xxx
- [24] *Ram Seshadri*, Current Opinion in Solid State and Materials Science 9 (2005) 1–7
- [25] *O. Oprea, E. Andronescu, B. S. Vasile, G. Voicu, C. Covaliu* - Digest Journal of Nanomaterials and Biostructures – 6(3), 1393-1401, 2011
- [26] *O. Oprea, O. R. Vasile, G. Voicu, L. Craciun, E. Andronescu* - Digest Journal of Nanomaterials and Biostructures – 7(4), 1757 - 1766, 2012
- [27] *O. R. Vasile, E. Andronescu, C. Ghitulica, B. S. Vasile, O. Oprea, E. Vasile, R. Trusca* – Journal of Nanoparticle Research, 14(12), 2012 doi: 10.1007/s11051-012-1269-7, 2012
- [28] *Xinyu Li, Shuxiang Wu, Ping Hu, Xiangjun Xing et al*, J. Appl. Phys. **106**, 043913 (2009);
- [29] *E.A. Gan'shina, A.B. Granovsky, A.F. Orlov, N.S. Perov, M.V. Vashuk*, Journal of Magnetism and Magnetic Materials. 321(7), 2009, 723–725

- [30] *A. Ianculescu, F. Prihor Gheorghiu, P. Postolache, O. Oprea, L. Mitoseriu* - Journal of Alloys and Compounds 504(2), 420-426, 2010 doi:10.1016/j.jallcom.2010.05.135
- [31] *D. Gingasu, O. Oprea, I. Mindru, D. C. Culita, L. Patron* - Digest Journal of Nanomaterials and Biostructures – 6(3), 1215 - 1226, 2011
- [32] *C.I. Covaliu, T. Mălăeru, G. Georgescu, O. Oprea, L. Alexandrescu, I. Jitaru* - Digest Journal of Nanomaterials and Biostructures, 6(4), 1491-1497, 2011
- [33] *C.I. Covaliu, L. C. Chioaru, L. Crăciun, O. Oprea, I. Jitaru* - Optoelectronics and Advanced Materials – Rapid Communications, 5 (10),1097-1102, 2011
- [34] *E. Andronescu, L. Bancu, T. Malaeru, I. Jitaru, Journal of Optoelectronics and Advanced Materials*, 9 (5), 2007
- [35] *J. Tauc, R. Grigorovici and A. Vancu*, Phys. Status Solidi **15** (1966), p. 627
- [36] *Sikhwivihilu, LM, Pillai, SK and Hillie, TK*. 2011, Journal of Nanoscience and Nanotechnology, Vol. 11(1-7), pp 1-7
- [37] *Tolstoy VP, Chernyshova IV, Skryshevsky VA*.2003. Handbook of Infrared Spectroscopy of Ultrathin Films, JOHN WILEY & SONS, INC, ISBN 0-471-35404-x
- [38] *Melghit K, Mohammed AK, Al-Amri I*, Materials Science and Engineering B 117 (2005) 302–306
- [39] *Amalric-Popescu D, Bozon-Verduraz F*, Today 70 (2001) 139–154
- [40] *Naoto Shirahata, Yoshitake Masuda, Tetsu Yonezawa, Kunihito Koumoto*, Langmuir 2002, 18, 10379-10385
- [41] *K. Gopinadhan*, Journal of Applied Physics 102, 113513, 2007
- [42] *Liping Kang, Menming Zhang, Zong-Huai Liu, Kenta Ooi*, Spectrochimica Acta Part A 67 (2007) 864–869
- [43] *M. Nakayama, C. Matsushima, K. Ogura*, Journal of Electroanalytical Chemistry 536 (2002) 47-53
- [44] *R. Kannan, A. Jegan, A. Ramasubbu, K. Karunakaran, S. Vasanthkumar*, Digest Journal of Nanomaterials and Biostructures Vol. 6, No 2, April - June 2011, p. 755 – 760